Available online at www.sciencedirect.com
SCIENCE DIRECT®
Journal of Organometallic Chemistry 691 (2006) 1498–1504
Journal of Organometallic Chemistry
www.elsevier.com/locate/jorganchem

Reactivity of di*tert*-butyldimethoxystannane with carbon dioxide and methanol: X-ray structure of the resulting complex

Danielle Ballivet-Tkatchenko *, Romain Burgat, Stéphane Chambrey, Laurent Plasseraud, Philippe Richard

Laboratoire de Synthèse et Electrosynthèse Organométalliques, UMR 5188 CNRS, Université de Bourgogne, 9 av A. Savary, BP 47870, 21078 Dijon Cedex, France

Received 4 November 2005; accepted 7 November 2005
Available online 19 December 2005

Abstract

The synthesis of dimethyl carbonate from carbon dioxide and methanol was studied with di*tert*-butyldimethoxystannane under pressure at temperatures ⩽423 K. The formation of dimethyl carbonate is accompanied by transformation of the stannane into a trinuclear complex, the structure of which has been determined by single-crystal X-ray diffraction technique. The relevance of this specie in the catalytic cycle is demonstrated by conducting recycling runs. A preliminary kinetic study underlines the steric influence of the *tert*-butyl ancillary ligands in the stabilisation of intermediates, by comparison with the *n*-butyl homologue.
© 2005 Elsevier B.V. All rights reserved.

Keywords: Carbon dioxide; Dimethyl carbonate; Dibutyldimethoxystannane; Supercritical fluids

1. Introduction

The conventional production of dimethyl carbonate involves the use of toxic phosgene or carbon monoxide rendering scale-up production problematic [1]. However, dimethyl carbonate (DMC) has low toxicity, rapid biodegradability [2], low impact on air quality [3], and new applications are foreseen in different sectors (e.g., polymers, fuels, organic synthesis) [4] provided friendly processes are available for its production. Accordingly, the three synthetic approaches currently under active scrutiny are: (i) carbonate transesterification, (ii) urea methanolysis, and (iii) methanol carbonation [5]. On a stoichiometric basis, the carbonation of methanol, so-called direct synthesis of DMC, is more attractive because atom economy [6] is highest, 83 wt%, forming only 17 wt% of water as the co-product (Eq. (1)).

$$CO_2 + 2CH_3OH \rightarrow (CH_3O)_2CO + H_2O \quad (1)$$

In addition, reaction (1) contributes to the direct fixation of carbon dioxide and to its use as renewable C_1 feedstock (i.e., recycling for producing chemicals), which is one of the current environmental challenges [7]. However, not surprisingly, carbon dioxide is much less reactive, and its transformation into organics is better achieved in the presence of catalysts.

It has been reported since now one decade that mono- and dialkyltin (IV) complexes [8] act as mediators for reaction (1) under solventless conditions with a positive effect of CO_2 pressure [9–11], taking, therefore, advantage of monophasic supercritical conditions [12]. These systems are selective in DMC but suffer from low activity. The reaction mechanism is poorly understood justifying further studies for improvement of catalyst design. We recently reported the CO_2 insertion into Sn–O bonds of di*n*-butyl(alkoxy)stannanes [11] and highlighted the role of distannoxanes [13]. In order to determine the influence of the *n*-butyl groups as ancillary ligands, we decided to shift

* Corresponding author. Tel.: +33 3 80 39 37 70; fax: +33 3 80 39 37 72.
E-mail address: ballivet@u-bourgogne.fr (D. Ballivet-Tkatchenko).

0022-328X/$ - see front matter © 2005 Elsevier B.V. All rights reserved.
doi:10.1016/j.jorganchem.2005.11.013

to more hindered ones which could stabilise different intermediate structures. The choice of *tert*-butyl ligands was motivated by the documented chemistry and structures in the di*tert*-butyltin (IV) series [14]. Of note, the first CO_2 adduct has been very recently characterised from a reaction involving (*tert*-$Bu_2SnO)_3$ [15].

In this paper, we focus on the reactivity of *tert*-$Bu_2Sn(OMe)_2$ (**1**) with CO_2 at atmospheric pressure and low temperature, then on DMC formation according to Eq. (1) under catalytic conditions using CO_2 as solvent and reagent. A preliminary kinetic study is also reported for comparison with *n*-$Bu_2Sn(OMe)_2$ (**2**) in order to investigate the steric control of the butyl groups. Characterisation of the organometallics were performed by volumetric CO_2 uptake and multi-nuclear magnetic resonance (NMR) and infrared (IR) spectroscopies. The solid-state structure of [OC(OSn*tert*-$Bu_2)_2O \cdot$ *tert*-$Bu_2Sn(OH)_2$] (**3**) was established by single-crystal X-ray diffraction analysis.

2. Results and discussion

2.1. Reaction under atmospheric CO_2 pressure

As neat liquid, the $^{119}Sn\{^1H\}$ NMR spectrum of **1** displays a singlet at δ −109 in agreement with a previous study [16]. Such a chemical shift value, within the range of five-coordinated tin nucleus [17], indicates either a dimeric or trimeric structure (Fig. 1) as for $[(CH_3)_2Sn(OCH_3)_2]_2$ or (*tert*-$Bu_2SnO)_3$, respectively [10,18]. In the IR spectrum, one ν(CH) stretching band for the methoxy groups is centred at 2804 cm^{-1} (Fig. 2(a)).

Under atmospheric CO_2 pressure, volumetric experiments on **1** (neat sample) led to a CO_2 uptake with a CO_2:Sn molar ratio of 0.70, at room temperature. Lowering the temperature to 273 K induced a slight increase to 0.80. Under the same experimental conditions, a toluene solution of **1** (1 M) provided CO_2:Sn ratios of 0.40 and 0.60 at room temperature and 273 K, respectively. The reaction was found reversible giving back the NMR and IR fingerprints of **1**, after 1 h in vacuo at room temperature. Comparison with the *n*-butyl analogue **2** points out that a definite CO_2:Sn stoichiometry is not reached [11]. In agreement, the NMR study of **1** under CO_2 revealed the formation of several species, some of them being under a dynamic exchange. When the neat transparent liquid **1** was submitted to an atmospheric pressure of CO_2 overnight, at room temperature, it was transformed into a white gel soluble in $CDCl_3$ displaying in the $^{119}Sn\{^1H\}$ spectrum

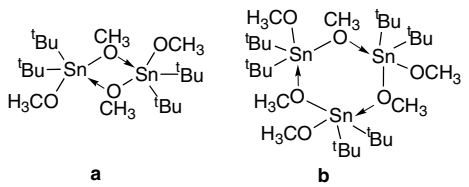

Fig. 1. Proposed dimeric and trimeric molecular structures for **1**.

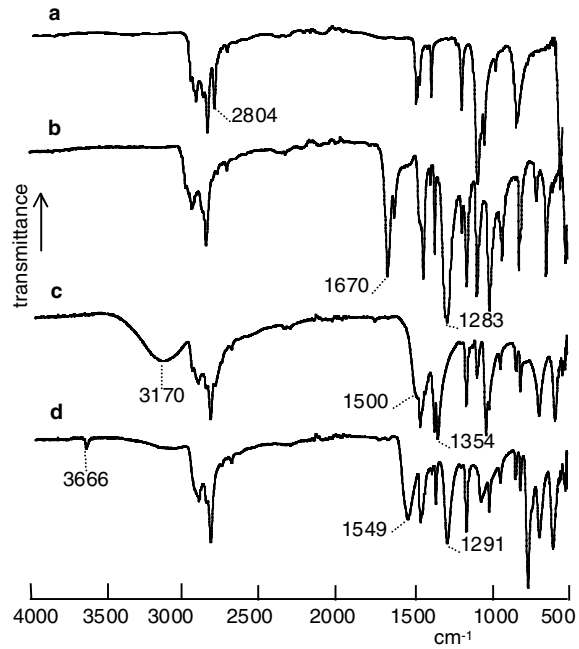

Fig. 2. IR(ATR) spectra of neat samples in the *tert*-butyl series: (a) **1**, (b) **1** after exposure to CO_2, (c) **3** · $3CH_3OH$, and (d) **3**.

the singlet of **1** accompanied by a broad signal at δ −163 and two other singlets at −282 and −302. Interestingly, enough, these two singlets are in a 1:2 ratio (relative integration), with tin-coupling satellites featuring a trinuclear species with two tin environments: δ −282 ($^2J^{119}Sn$, $^{119,117}Sn = 94$) and δ −302 ($^2J^{119}Sn$, $^{117}Sn = 195$, $^2J^{119}Sn$, 119,117Sn = 94). Therefore, this species is probably reminiscent of the trimeric structure **1b** in which two of the three terminal methoxy ligands have been carbonated (CO_2:Sn = 0.67). The temperature dependence of the $^{119}Sn\{^1H\}$ NMR spectrum indicates the occurrence of several species at 273 K, some of them being under dynamic exchange (Fig. 3). Finally, at 233 K, one predominant

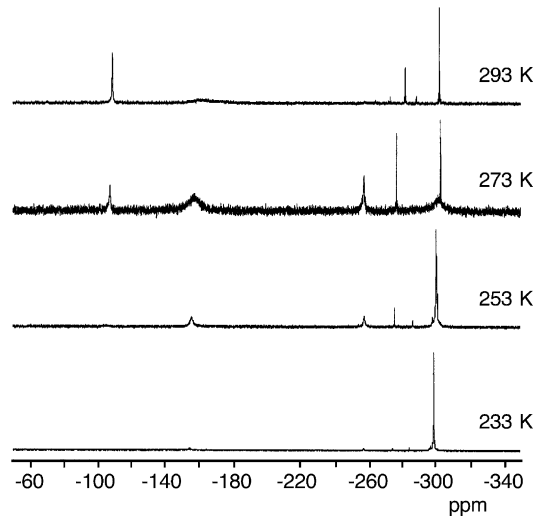

Fig. 3. Temperature dependence of the $^{119}Sn\{^1H\}$ NMR spectrum of **1** under CO_2 in $CDCl_3$ solution.

signal is present at δ −299, whilst the $^{13}C\{^1H\}$ NMR spectrum reveals two methoxy signals of equal intensity at δ 53.97 and 57.30 and a carbonate signal at δ 157.86. The IR spectrum of carbonated **1** (neat) reported in Fig. 2(b) shows characteristic $\nu(CO_3)$ bands centred at 1670, 1627, and 1283 cm^{-1}. These values compare with those of the hemicarbonate moiety, Sn–OC(O)OCH_3, characterised for the dimethyl and di*n*-butyl analogues [10,11]. The reactivity of **1** with CO_2 under mild conditions led us to examine whether it is prone to form DMC under pressure and temperature.

2.2. DMC yield under CO_2 pressure

As **1** bears two methoxy ligands per tin, it was relevant to investigate the stoichiometric formation of DMC with temperature under CO_2 pressure in toluene. The behaviour of **2**, the homologous *n*-$Bu_2Sn(OCH_3)_2$ stannane, was also examined for the steric role of the butyl ligands. A reaction temperature screening revealed that **1** and **2** are prone to give DMC. The onset of detectable DMC was located at 355 K. Interestingly, a different reaction stoichiometry was evidenced for the two complexes. The maximum DMC:Sn molar ratio that could be obtained was ~0.3 and 0.5 for **1** and **2**, respectively. Whilst **2** was quantitatively transformed into the distannoxane [*n*-$Bu_2(CH_3O)Sn]_2O$ [13], we found that **1** gave a mixture of three species when running $^{119}Sn\{^1H\}$ experiment in $CDCl_3$ (δ −84, −109, and −113; integral ratio 1:4:2). The $^{13}C\{^1H\}$ spectrum revealed three signals for the Sn–*C* and C*C*H_3 carbons, respectively, and two methoxy resonances at δ 54.71 and 53.90. Accordingly, two species have been identified as **1** and (*tert*-$Bu_2SnO)_3$. The third one had characteristic resonances at δ_{Sn} −113 with $^2J^{119}Sn,^{117}Sn$ value of 928, $\delta_{C-(CH_3)_3}$ at 38.86 ($^1JC-^{119,117}Sn = 497$, 475) and δ_{OCH_3} at 53.90. Bearing methoxy ligands, this specie is tentatively assigned to the distannoxane [*tert*-$Bu_2(CH_3O)Sn]_2O$ that disproportionates to some extent in solution giving **1** and (*tert*-$Bu_2SnO)_3$. Precedents on the instability of other distannoxanes in the *tert*-butyl series can be found in the recent literature [19]. Nonetheless, these observations underline the role of the butyl ligands in the stabilisation of intermediates when DMC is formed. The kinetics was also found to be different. Fig. 4 shows typical profiles of DMC yield versus time at 9 MPa CO_2 pressure for two temperatures.

During the first hours of a run, the reaction rate was constant that allows to get accuracy in initial r_0 determinations (at $t = 0$). The r_0 values reflect the intrinsic reactivity of the starting complexes for DMC formation because secondary reactions, if any, are negligible. At 371 K, r_0 values of 0.041 and 0.14 mmol g^{-1} h^{-1} were obtained for **1** (hollow circles) and **2** (filled circles), respectively. This result points out that the reaction is much slower with the *tert*-butyl complex. At 386 K, **2** (filled squares) behaves normally with rate acceleration at higher temperature ($r_0 = 0.45$ mmol g^{-1} h^{-1}). In contrast, **1** (hollow squares)

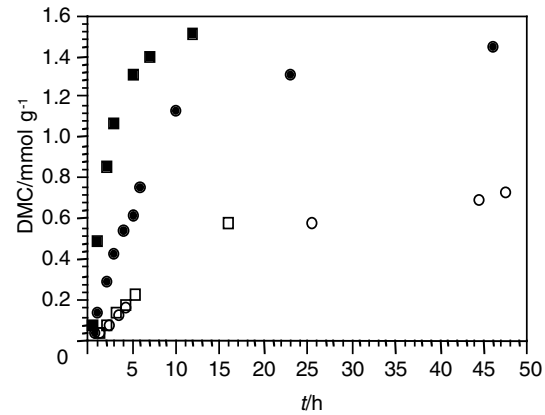

Fig. 4. Effect of reaction time on DMC yield with **1** and **2** under 9 MPa CO_2 pressure at 371 K [**1** (○), **2** (●)] and 386 K [**1** (□), **2** (■)] (**1**, **2** = 0.44 g, toluene = 9 cm^3, CO_2 = 10.2 g).

exhibits a negligible enhancement ($r_0 = 0.046$ mmol g^{-1} h^{-1}) pointing out that the *tert*-butyl complex is not only different in DMC:Sn stoichiometry but also with temperature. This effect could be indicative of a decrease in tin species prone to form DMC due to equilibrium between monomeric and active oligomeric species. Further work is in progress to correlate the reactivity with the nuclearity in comparison with **2**.

Replacing toluene for methanol was further examined to assess the catalytic activity from precursor **1** (Eq. (1)). When a methanolic solution of **1** (0.2 M) was submitted to 20 MPa of CO_2 for 14 h at 423 K [20], DMC was formed in the molar ratio DMC:Sn = 0.54. The IR spectrum of the white powder collected after depressurisation and elimination of the volatiles showed the disappearance of the ν(CH) band characteristic of the methoxy groups whilst those of *tert*-butyl groups were still present together with new strong bands centred at 1500 and 1354 cm^{-1} assigned to a CO_3^{2-} moiety [21]. In addition, a broad band at 3170 cm^{-1} was indicative of hydrogen-bonding. The white powder was insoluble in common organic solvents, rendering its analysis problematic by NMR in solution. Interestingly, enough, this tin-based powder was active and selective for DMC synthesis when re-engaged for successive catalytic runs.

Typically, at the end of the catalytic run with **1** (4 mmol), depressurisation followed by elimination of the organics left a tin-based residue which was weighed and re-introduced into the reactor for a new run under the same experimental conditions. The procedure was repeated three more times. The corresponding DMC yields, expressed in mmol per gram of tin compound, are reported in Fig. 5. The recycling experiments led to lower DMC yields than with the fresh stannane whereas no activity was found in the absence of tin-based compounds. As water is co-produced during the reaction, one can speculate that it may poison the active sites. This was demonstrated by conducting an experiment in the presence of 2,2-dimethoxypropane (Fig. 5, run 6) for acting as a water-trap in being hydrolysed to acetone and methanol [22].

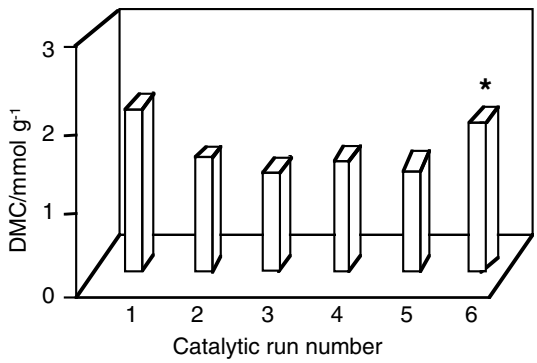

Fig. 5. DMC yield vs. number of recyclings from **1** under 20 MPa CO_2 pressure for 14 h at 423 K. (**1** = 1.5 g, CH_3OH = 20 cm^3, *: addition of 16 mmol of 2,2-dimethoxypropane).

For clarity, the abbreviation used in the following for the recycled tin-based compound will be **REC-1**. Its dissolution in methanol after work-up of the solution obtained from run 5 (Fig. 5) gave, within few days at room temperature, single-crystals suitable for X-ray crystallographic structure determination.

2.2.1. X-ray structure and spectroscopic characterisation of [OC(OSntert-Bu$_2$)$_2$O · tert-Bu$_2$Sn(OH)$_2$] (3)

The molecular structure of **3** is shown in Fig. 6. Selected bond distances and angles are reported in Table 1. Compound **3** is a trinuclear cluster; each tin atom have two *tert*-butyl ligands highlighting that the Sn–C(sp^3) bonds are stable under the catalytic conditions. The structure can be viewed as being derived from the incorporation of a carbonate fragment, CO_3^{2-}, to a planar Sn_3O_3 core, building an eight-membered Sn_3CO_5 ring with a central μ_3-O atom. The two μ_2-oxygen atoms of the Sn_3O_3 core arise from two bridging hydroxyl groups revealing the *tert*-$Bu_2Sn(OH)_2$ sub-unit. The tin atoms are pentacoordinated in a distorted trigonal bipyramidal arrangement (TBP). The equatorial plane contains the *tert*-butyl groups (C–Sn–C = 120(1)°, mean) and the μ_3-O atom (C–Sn–O(μ_3) = 120(6)°, mean). The axial positions are occupied by the oxygen atoms of the hydroxy and carbonate groups with bond angles smaller than 180°: O(2)–Sn(1)–O(3) = 143.47(15)°, O(2)–Sn(2)–O(4) = 156.29(5)°, and O(3)–Sn(3)–O(5) = 154.85(16)°. The carbonate ligand is linked to two tin atoms of the Sn_3O_3 core in the η^1,η^1 coordination mode. Moreover, it exhibits a rigorous planar trigonal geometry (O–C–O = 120.0(7)°, mean). The mean plane of the CO_3 moiety is tilted with respect to the six-atoms Sn_3O_3 mean plane (RMS deviation = 0.046 Å) by 26.6(2)°, leading to a *anti,anti* conformation. Such a conformation is encountered in many solid-state structures of transition metal carbonate complexes, especially for iron [23], chromium [24], molyb- denum [25], vanadium [26], and copper [27].

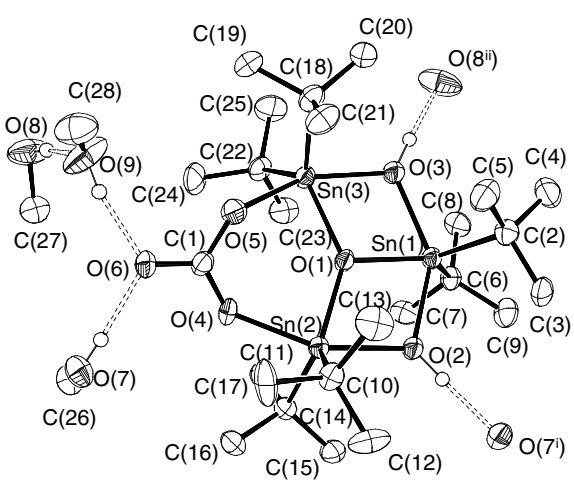

Fig. 6. ORTEP representation of **3** · $3CH_3OH$ with the atom-labelling scheme (50% probability ellipsoids). H atoms are not shown for clarity except those engaged in hydrogen bonding. Symmetry operations used to generate equivalent atoms: i = $x - 1/2$, y, $1/2 - z$; ii = $x + 1/2$, $1/2 - y$, $-z$.

The closer chemically related structures that have been published correspond to the compounds [$R_2Si(OSn$*tert*-$Bu_2)_2O$(*tert*-$Bu_2Sn)(OH)_2$] (R = CH_3, Ph) [16,28]. The Sn_3O_3 core are also almost planar. All Sn–O bonds from the three-coordinate oxygen to tin are equivalent and short (ca. 2.09 Å). The difference with **3** resides in the Sn(2)–O(1) and Sn(3)–O(1) bond lengths which are even shorter 2.048(4) and 2.059(4) Å, respectively. The other dissimilarity arises in the two Sn–O(H) bond distances for the bridging hydroxyl groups. They are more symmetrical in **3**, ca. 2.16 than for the siloxane derivatives ca. 2.27 and 2.10 Å. This general trend on both Sn-(μ_3-O) and Sn–O(H) bond distances variations has been very recently reported for the ionic complex [$Ph_2P(OSn$*tert*-$Bu_2)_2O$ · *tert*-$Bu_2Sn(OH)_2$][O_3SCF_3] [29]. Notable in the structure is the presence of intermolecular hydrogen bonding between the hydroxy protons and one oxygen atom of the O_3SCF_3 groups, giving rise to the formation of an infinite chain in the crystal lattice. Compound **3** also experiences intermolecular hydrogen bonding with three independent methanol molecules forming a 2D-infinite network of superposed pleated sheets. The hydrogen bonding modes are best viewed in Fig. 7. The uncoordinated O(6) atom of the CO_3^{2-} group is hydrogen bonded to two methanol molecules with O(6)···O(7) and O(6)···O(9) distances of 2.673(7) and 2.638(8) Å, respectively. Then, these two methanol molecules are hydrogen bonded, respectively, to an OH group of a second unit (O(7)···O(2^i) = 2.722(6) Å) and to a methanol (O(9)···O(8) = 2.631(9) Å) which is further hydrogen bonded to an OH group of a third unit (O(8)···O(3^{iii}) = 2.700(7) Å). In summary, the hydrogen atoms involved in the network come from the OH groups of the two bridging hydroxyls and of the three methanol molecules, two of them being associated. Moreover, the uncoordinated oxygen atom (carbonyl function) exhibits two hydrogen bonds. The adduct will be referred to **3** · $3CH_3OH$ in the following.

Table 1
Selected bond distances (Å) and angles (°) for $\mathbf{3} \cdot 3CH_3OH$

Sn(1)–O(1)	2.080(4)	Sn(2)–O(1)	2.048(4)	Sn(3)–O(1)	2.059(4)
Sn(1)–O(2)	2.136(4)	Sn(2)–O(2)	2.167(4)	Sn(3)–O(3)	2.164(4)
Sn(1)–O(3)	2.139(4)	Sn(2)–O(4)	2.140(4)	Sn(3)–O(5)	2.119(4)
Sn(1)–C(2)	2.185(6)	Sn(2)–C(14)	2.169(6)	Sn(3)–C(18)	2.180(7)
Sn(1)–C(6)	2.189(6)	Sn(2)–C(10)	2.169(6)	Sn(3)–C(22)	2.175(6)
C(1)–O(6)	1.266(7)	C(1)–O(4)	1.280(7)	C(1)–O(5)	1.310(7)
O(2)···O(7^{i})	2.722(6)	O(6)···O(7)	2.673(7)	O(3)···O(8^{ii})	2.700(7)
O(6)···O(9)	2.638(8)	O(8)···O(9)	2.631(9)		
O(1)–Sn(1)–O(2)	71.92(15)	O(1)–Sn(2)–O(4)	85.83(15)	O(1)–Sn(3)–O(5)	86.15(15)
O(1)–Sn(1)–O(2)	71.92(15)	O(1)–Sn(2)–O(4)	85.83(15)	O(1)–Sn(3)–O(5)	86.15(15)
O(1)–Sn(1)–O(3)	71.66(15)	O(1)–Sn(2)–O(2)	71.89(14)	O(1)–Sn(3)–O(3)	71.55(15)
O(2)–Sn(1)–O(3)	143.47(15)	O(4)–Sn(2)–O(2)	156.29(16)	O(5)–Sn(3)–O(3)	154.85(16)
O(6)–C(1)–O(4)	120.3(6)	O(6)–C(1)–O(5)	119.0(5)	O(4)–C(1)–O(5)	120.6(5)

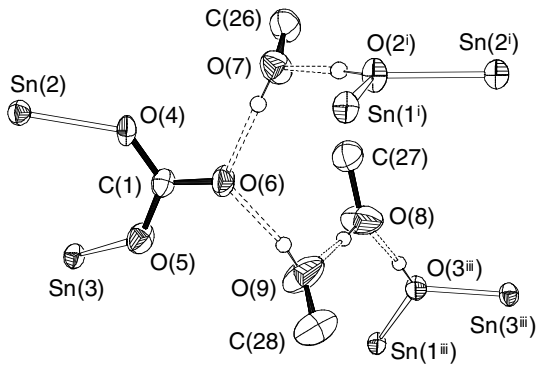

Fig. 7. ORTEP representation of the hydrogen bonding in the crystal lattice of $\mathbf{3} \cdot 3CH_3OH$ with the atom-labelling scheme (50% probability ellipsoids). The other H atoms are not shown for clarity. Symmetry operations used to generate equivalent atoms: i = $x - 1/2$, y, $1/2 - z$; iii = $x - 1/2$, $1/2 - y$, $-z$.

The IR spectrum of $\mathbf{3} \cdot 3CH_3OH$ (Fig. 2(c)) is identical to that of **REC-1**. The characteristic broad ν(O–H···O) band is at ca. 3170 cm^{-1} whilst the $\nu(CO_3)$ bands are centred at 1500 and 1354 cm^{-1}. Methanol could be removed from the lattice by overnight vacuum treatment at room temperature. The IR spectrum of the left white powder revealed the expected shifts for the hydroxyl groups, 3666 cm^{-1}, and for the carbonate, 1549 and 1291 cm^{-1} (Fig. 2(d)). Identical drying procedure applied to **REC-1** led to the same IR fingerprint. More significant, the elemental analysis nicely corresponded to the molecular formula of **3**, demonstrating that the crystallised compound is not a side-product, but the resting specie responsible for DMC formation under the recycling protocol.

In spite of the poor solubility of **3**, a $^{119}Sn\{^1H\}$ experiment of a dilute $CDCl_3$ solution could be run. The spectrum showed the notable appearance of $(tert\text{-}Bu_2SnO)_3$ at δ −83 accompanied by two other resonances at δ −267 and −297 (1:2 ratio) which are tentatively assigned to the two tin environments of **3**. It is noteworthy, that a $CDCl_3$ solution of $[Ph_2Si(OSn\,tert\text{-}Bu_2)_2O \cdot tert\text{-}Bu_2Sn(OH)_2]$ has been reported to contain $(tert\text{-}Bu_2SnO)_3$ [16]. The proposed mechanism, which involves the dissociation of the $tert\text{-}Bu_2Sn(OH)_2$ sub-unit and its further dehydration to $(tert\text{-}Bu_2SnO)_3$, may therefore also take place with **3**.

The transformation of **1** into **REC-1**, the structure of which corresponds to $\mathbf{3} \cdot 3CH_3OH$ involves the substitution of the methoxy groups by OH, carbonate and oxo ligands with the concomitant formation of DMC. Such rearrangement of the tin coordination spheres leads to the $(tert\text{-}Bu_2Sn)_2(CO_3)O$ and $tert\text{-}Bu_2Sn(OH)_2$ sub-units which suggests that CO_2 and water, the co-product of reaction (1), plays a crucial role in the stabilisation of this trinuclear complex. Possibly the reaction occurs stepwise with the intermediate formation of $(tert\text{-}Bu_2SnO)_3$, because this complex was reported to afford **3** in acetone when treated with an aqueous solution of Na_2CO_3 [30]. The presence of OH groups corroborates the dehydrating role of 2,2-dimethoxypropane for the increase of DMC yield (Fig. 5).

3. Conclusions

The present approach answers some key issues for designing more active organotin (IV) catalysts for the direct synthesis of dimethyl carbonate from carbon dioxide and methanol. The structural elucidation of a key intermediate, characterised as an hexa*tert*-butyltritin complex, constitutes a significant outcome towards the identification of the active species under working conditions. Recycling protocol demonstrates the reversible poisoning of the active centres by water, the co-product of the reaction. Moreover, this work highlights, for the first time, that dibutyldimethoxystannanes are prone to form dimethyl carbonate in the absence of methanol, on a stoichiometric basis, at much lower temperature. The steric influence of the ligands, *tert*- versus *n*-butyl, governs the kinetics providing evidence for different rate-determining step(s) and, therefore, overall reaction scheme. Thus, the judicious choice of ancillary ligands can be exploited to control the number of active sites through the stabilisation of intermediates of different nuclearities. Future work will aim to establish the rate equations and to assess the role of methanol under catalytic conditions.

4. Experimental

4.1. General

All manipulations were carried out by using standard Schlenk tube techniques. Toluene and methanol (Carlo Erba, RPE grade) were dried and distilled under argon from CaH_2 and $Mg(OCH_3)_2$, respectively. Carbon dioxide N45 TP was purchased from Air Liquide and used without further purification. The compound *tert*-Bu_2SnCl_2 was synthesised from $SnCl_4$ according to a published method [31]. The ^1H, $^{13}C\{^1H\}$ and $^{119}Sn\{^1H\}$ NMR experiments were run on a Bruker Avance 300 spectrometer at 295 K unless otherwise stated; *J* values are given in Hz. IR spectra were recorded on a Bruker Vector 22 equipped with a Specac Golden Gate™ ATR device. Elemental analysis was performed at the Laboratoire de Synthése et Electrosynthése Organométalliques, Université de Bourgogne, Dijon.

4.2. Synthesis of tert-$Bu_2Sn(OMe)_2$ (**1**)

A solution of *tert*-Bu_2SnCl_2 (8.478 g, 28 mmol) in toluene (40 cm^3) was added dropwise, to a solution of CH_3ONa (58 mmol) in methanol at room temperature. The suspension was stirred overnight, after which it was filtrated. The solution was evaporated under reduced pressure to leave a yellow viscous oil, which was purified by vacuum distillation at 309 K to give **1** (6.295 g, 76%) as a colourless oil (Found: C, 40.79; H, 8.09. $C_{10}H_{24}O_2Sn$ requires C, 40.71; H, 8.20%).

IR (neat film, cm^{-1}): 2922, 2847, 2823, 2803, 1467, 1366 and 1064; ^1H NMR (300 MHz, $CDCl_3$, Me_4Si): δ (ppm) = 1.36 (9H, quintet, ^3JH, ^{119,117}Sn 92 and 87, $SnC(CH_3)_3$), 3.80 (3H, singlet, O–CH_3); ^{119}Sn NMR (111.9 MHz, $CDCl_3$, Me_4Sn): δ (ppm) = −109 (^1JSn–Cα 471); ^{13}C NMR (75.4 MHz, $CDCl_3$, Me_4Si): δ (ppm) = 29.70 (C–CH_3), 39.28 (^1JC–^{119,117}Sn 471 and 450, *C*–CH_3), 54.51 (O–CH_3).

4.3. Gasometry

A Schlenk tube containing **1** (0.295 g, 1 mmol) as neat or in toluene (1 cm^3) was connected to a pressure transducer and to a CO_2 reservoir of known pressure and volume, maintained at 295 K. The amount of CO_2 adsorbed was calibrated by reference experiments. The calculated CO_2:Sn molar ratio was at ±0.05.

4.4. Catalytic experiments

Caution: When high pressures are involved, appropriate safety precautions must be taken.

In a typical experiment under CO_2 pressure, 20 cm^3 of methanol or toluene were added to the tin compound (4 mmol based on tin) in a Schlenk tube. Then, the solution was transferred into a 120 cm^3 stainless steel batch reactor. Finally, CO_2 was introduced at 4 MPa, at room temperature. The reactor was heated up to 423 K (controlled by an internal thermocouple) and the pressure was adjusted to the desired value by a high-pressure CO_2 pump (Top Industrie S.A., France). After 14 h of reaction under magnetic stirring, the autoclave was cooled down to 273 K, depressurised and the condensed phase transferred to a Schlenk tube. Trap-to-trap vacuum distillation at room temperature allowed to separate the organics which were analysed by GC using toluene as reference (Fisons 8000, J&W Scientific, DB-WAX 30 m capillary column, FID detector), and the tin residue was characterised by multinuclear NMR and IR. Recycling experiments consisted in taking the tin residue for successive catalytic runs under the same experimental conditions.

For the kinetic experiments, a 56 cm^3 reactor was used and charged with a 9 cm^3 toluene solution of **1** or **2** (1.5 mmol of the monomers). A sampling valve (0.090 mL) allowed to follow the DMC yield with time. At the end of the experiment, the aforementioned degassing and analytical procedures were adopted. Before quenching the reaction at 273 K, a last sampling allowed to check consistency between the two analytical procedures; the fit was better than 3% (relative error).

4.5. Characterisation of **REC-1**

The tin-based residue collected after the fourth recycling experiment from **1** was dried overnight in vacuo at room temperature and characterised as **3** (Found: C, 37.24; H, 7.22. $C_{25}H_{56}O_6Sn_3$ requires C, 37.12; H, 6.98%); IR (neat solid, cm^{-1}): 3666, 2925, 2846, 1549, 1468, 1365, 1290.

4.6. Crystal structure determination for **3** · $3CH_3OH$

Colourless prismatic single-crystals of [OC(OSn*tert*-$Bu_2)_2O$ · *tert*-$Bu_2Sn(OH)_2$] · $3CH_3OH$ were grown from a methanolic solution at room temperature. Diffraction data were collected from a suitable crystal (0.2 × 0.2 × 0.2 mm) on a Nonius Kappa CCD (Mo Kα radiation, λ = 0.71073 Å). The structure was solved using a Patterson search program and refined with full-matrix least-squares methods based on F^2 (SHELX-97) [32] with the aid of the WINGX program [33]. All non-hydrogen atoms were refined with anisotropic thermal parameters. Hydrogen atoms were included in their calculated positions or found in the final difference Fourier maps and refined with a riding model. One of the *tert*-butyl groups is disordered and was refined over two positions with multiplicity converged to [0.66(3)/0.34(3)].

Crystal data. $C_{25}H_{56}O_6Sn_3 \cdot 3(CH_4O)$, M = 904.95 g mol^{-1}, orthorombic, a = 18.5654(5) Å, b = 17.6822(5) Å, c = 24.2930(7) Å, V = 7974.8(4) $Å^3$, T = 110 K, space group *Pbca* (no. 61), Z = 8, μ(Mo Kα) = 1.905 mm^{-1}, 23423 reflections measured, 8431 unique (R_{int} = 0.053) which were used in all calculations. The final $R(F)$ and $wR(F^2)$ were 0.127 and 0.067 (all data), respectively; number of parameters = 402.

5. Supplementary material

Crystallographic data for the structure reported in this paper have been deposited at the Cambridge Crystallographic Data Center, CCDC, No. CCDC 278211 for $[OC(OSn\textit{tert}\text{-}Bu_2)_2O \cdot \textit{tert}\text{-}Bu_2Sn(OH)_2] \cdot 3CH_3OH$. Copies of the data may be obtained free of charge from The Director, CCDC, 12 Union Road, Cambridge CB2 1EZ, UK (fax: int. code +44 1223 336 033; e-mail: deposit@ccde.cam.ac.uk or www: http://www.ccdc.cam.ac.uk).

Acknowledgements

We are grateful for the financial support of this work received from the Centre National de la Recherche Scientifique and from the Ministère de la Recherche (S.C., doctoral grant).

References

[1] Société Nationale des Poudres et Explosifs, FR 2163884, 1973;
D. Delledonne, F. Rivetti, U. Romano, Appl. Catal. A 221 (2001) 241;
S. Uchiumi, K. Ataka, T. Matsuzaki, J. Organomet. Chem. 576 (1999) 279.
[2] F. Rivetti, U. Romano, D. Delledonne, in: P.T. Anastas, T.C. Williamson (Eds.), Green Chemistry, ACS Symposium Series, vol. 626, 1996, p. 70.
[3] Y. Katrib, G. Deiber, P. Mirabel, S. Le Calvé, C. George, A. Mellouki, G. Le Bras, J. Atmos. Chem. 43 (2002) 151.
[4] M. Ricci, in: M. Aresta (Ed.), Carbon Dioxide Recovery and Utilization, Kluwer Academic Publishers, Dordrecht, 2003, pp. 395–401, ch. 16;
M.A. Pacheco, C.L. Marshall, Energy Fuels 11 (1997) 2;
P. Tundo, M. Selva, Acc. Chem. Res. 35 (2002) 706.
[5] D. Ballivet-Tkatchenko, S. Sorokina, in: M. Aresta (Ed.), Carbon Dioxide Recovery and Utilization, Kluwer Academic Publishers, Dordrecht, 2003, pp. 261–277, ch. 10.
[6] B.M. Trost, Angew. Chem. Int. Ed. 34 (1995) 259.
[7] M. Aresta, A. Dibenedetto, Catal. Today 98 (2004) 455.
[8] Mono- and dialkyl tin (IV) compounds are largely used as stabilisers and catalysts in the sector of polymers. In Europe, 60% of the production is for food packaging and 40% for technical applications. They are not listed in Annex I of the Dangerous Substances Directive (67/548/EEC)..
[9] J. Kizlink, I. Pastucha, Collect. Czech. Chem. Commun. 6 (1995) 687.
[10] J.-C. Choi, T. Sakakura, T. Sako, J. Am. Chem. Soc. 121 (1999) 3793.
[11] D. Ballivet-Tkatchenko, O. Douteau, S. Stutzmann, Organometallics 19 (2000) 4563.
[12] E.J. Beckman, J. Supercrit. Fluids 28 (2004) 121.
[13] D. Ballivet-Tkatchenko, T. Jerphagnon, R. Ligabue, L. Plasseraud, D. Poinsot, Appl. Catal. A 255 (2003) 93.
[14] J. Beckmann, K. Jurkschat, Coord. Chem. Rev. 215 (2001) 267.
[15] J. Beckmann, D. Dakternieks, A. Duthie, N.A. Lewcenko, C. Mitchell, Angew. Chem. Int. Ed. 43 (2004) 6683.
[16] J. Beckmann, K. Jurkschat, B. Mahieu, M. Schürmann, Main Group Met. Chem. 21 (1998) 113.
[17] P.J. Smith, A.P. Tupciauskas, Ann. Rep. NMR Spectrosc. 8 (1978) 291.
[18] H. Puff, W. Schuh, W. Sievers, W.R. Wald, R. Zimmer, J. Organomet. Chem. 260 (1984) 271.
[19] D. Dakternieks, K. Jurkschat, S. van Dreumel, E.R.T. Tiekink, Inorg. Chem. 36 (1997) 2023;
M. Biesemans, G. Buytaert, L. Van Lokeren, J.C. Martins, R. Willem, E.R.T. Tiekink, Organometallics 22 (2003) 1888.
[20] The reaction pressure was set at 20 MPa for which the highest DMC yield was obtained with **2**. Visual checking with a reactor equipped with sapphire windows indicated that the reaction medium was monophasic.
[21] B.Y.K. Ho, J.J. Zuckerman, J. Organomet. Chem. 96 (1975) 41.
[22] T. Sakakura, J.-C. Choi, Y. Saito, T. Masuda, T. Sako, T. Oriyama, J. Org. Chem. 64 (1999) 4506.
[23] D.L. Jameson, C.-L. Xie, D.N. Hendrickson, J.A. Potenza, H.J. Schugar, J. Am. Chem. Soc. 109 (1987) 740;
S. Drueke, K. Wieghardt, B. Nuber, J. Weiss, Inorg. Chem. 28 (1989) 1414;
N. Arulsamy, D.J. Hodgson, J. Glerup, Inorg. Chim. Acta 209 (1993) 61;
T. Fujita, S. Ohba, Y. Nishida, A. Goto, T. Tokii, Acta Crystallogr., Sect. C 50 (1994) 544;
N. Arulsamy, P.A. Goodson, D.J. Hodgson, J. Glerup, K. Michelsen, Inorg. Chim. Acta 216 (1994) 21;
W. Schmitt, C.E. Anson, R. Sessoli, M. van Veen, A.K. Powell, J. Inorg. Biochem. 91 (2002) 173.
[24] K. Wieghardt, W. Schmidt, R. Van Eldik, B. Nuber, J. Weiss, Inorg. Chem. 19 (1980) 2922;
L. Spiccia, G.D. Fallon, A. Markiewicz, K.S. Murray, H. Riesen, Inorg. Chem. 31 (1992) 1066;
X.-Y. Chen, J. Xia, B. Zhao, P. Cheng, S.-P. Yan, D.-Z. Liao, Z.-H. Jiang, H.-B. Song, H.-G. Wang, J. Coord. Chem. 57 (2004) 231.
[25] M.J. Manos, A.D. Keramidas, J.D. Woolins, A.M.Z. Slawin, T.A. Kabanos, J. Chem. Soc., Dalton Trans. (2001) 3419.
[26] T.C.W. Mak, P.-J. Li, C.-M. Zheng, K.-Y. Huang, J. Chem. Soc., Chem. Commun. (1986) 1597.
[27] B.F. Abrahams, M.G. Haywood, R. Robson, Chem. Commun. (2004) 938.
[28] F. Cervantes-Lee, H.K. Sharma, I. Haiduc, K.H. Pannell, J. Chem. Soc., Dalton Trans. (1998) 1.
[29] J. Beckmann, D. Dakternieks, A. Duthie, K. Jurkschat, M. Mehring, C. Mitchell, M. Schürmann, Eur. J. Inorg. Chem. (2003) 4356.
[30] H. Reuter, Ph.D. Thesis, University of Bonn, 1987.
[31] S.A. Kandil, A.L. Allred, J. Chem. Soc. A (1970) 2987.
[32] G.M. Sheldrick, SHELX-97 (includes SHELXS-97 and SHELXL-97), Release 97-2, Programs for Crystal Structure Analysis, University of Göttingen, Göttingen, Germany, 1998.
[33] L.J. Farrugia, J. Appl. Crystallogr. 32 (1999) 837.